Multistate Latching MEMS Variable Optical Attenuator

R. R. A. Syms, H. Zou, J. Stagg, and D. F. Moore

***Abstract*—A multistate latching variable optical attenuator (VOA) is demonstrated using microelectromechanical systems (MEMS) technology. The mechanism is used to fix the position of a shutter inserted into the optical path between two single-mode fibers. The mechanism and fiber mounts are fabricated in 85 μm thick silicon using bonded silicon-on-insulator material, by deep reactive ion etching. The device can be continuously adjusted or latched into a discrete set of attenuation states using a rack-and-tooth mechanism driven by electrothermal shape bimorph actuators. Electromechanical and optical characterization is performed to demonstrate a latching VOA function, with a maximum attenuation of 30 dB.**

***Index Terms*—Microelectromechanical systems (MEMS), microoptoelectromechanical systems (MOEMS), variable optical attenuator (VOA).**

VARIABLE OPTICAL ATTENUATORS (VOAs) based on insertion of a shutter into an optical beam have been fabricated using microelectromechanical systems (MEMS) technology, with electrostatic, electromagnetic and electrothermal actuation [1]–[3]. Often, it is desirable to be able to set the attenuation, and hold this state even after removal of electrical power; however, few demonstrated devices have offered a latching function. One example is a VOA with an elastic clamp [4]. Rack-and-tooth mechanisms [5] are potentially more resistant to vibration and shock, but their resolution is limited by the minimum tooth size and by any clearances. For example, using fabrication by deep reactive ion etching (DRIE) of bonded silicon-on-insulator (BSOI), the resolution is insufficient for direct operation of a VOA.

In this letter, we demonstrate a simple solution for a rugged, multistate latching MEMS VOA. First, we note that positional resolution may be increased with mechanical levers, as shown in Fig. 1. Here a lever of length L hinged at its base by flexures may be rotated to adjust the position Y of a single tooth at its free end. This tooth engages with a rack mounted on a second lever, which is also hinged at its base by flexures so that it may perform clamp and release operations. If the tooth spacing of the rack is Δ, and the flexures act as perfect hinges, the position y at a point L' along the lever may be adjusted in increments of $\Delta L'/L$. With a tooth spacing of (say) $\Delta = 10$ μm, and $L/L' = 10$, y may be adjusted in increments of 1 μm. This resolution is sufficient to allow different attenuation states to be achieved by insertion of a shutter into the path of the optical beam from a single-mode fiber.

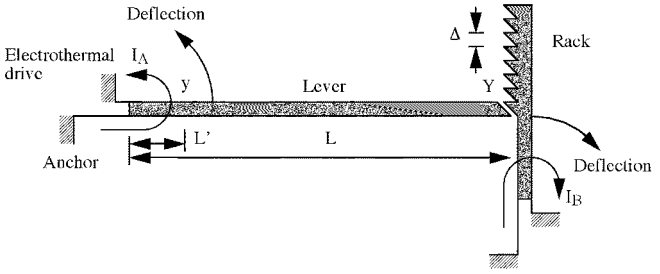

Fig. 1. Rack and tooth latch mechanism based on electrothermal shape bimorph actuators.

Crucial to this design is a simple flexure mechanism that allows the two components to be rotated under electrical control, and which does not suffer from otherwise unwanted deflections. The electrothermal shape bimorph actuator of Guckel [6] is one possibility. The device consists of a U-shaped structure suspended on two points, which may be heated by passing a current between the anchors. Asymmetries between the arms then result in differences in local temperature, which in turn causes differential thermal strains. The asymmetries may result from variations in width along two arms of similar length, or differences in length. These strains deflect and rotate the free end of the device. With careful design, either the linear or the angular component may be enhanced [7]. To enhance the latter, differences in arm length are more appropriate than variations in arm width [8]. Fig. 1 shows two electrothermal actuators with unequal arms. When heating currents I_A and I_B are applied, the longer arms expand preferentially to deflect the lever and rack in the directions shown. Importantly, similar deflections may also be sustained by purely mechanical loading, allowing a latched deflection to be retained after removal of power.

Fig. 2 is a schematic (not to scale) of a VOA based on this principle. The mechanism is fabricated by single-layer patterning, together with alignment features consisting of spring clips, each of length 1 mm and width 20 μm, which are deflected by 10 μm when standard 8/125 μm telecom fibers are inserted [1]. The separation between the fiber ends is 50 μm. The shutter blade is angled, to direct the reflected light into the cladding of the input fiber, and its initial position is 10 μm from the optical axis. To reduce the rotation of the shutter that accompanies translation, it is mounted on a second lever, hinged at its base by a flexure and connected to the main lever by a link bar, also hinged by flexures.

Manuscript received July 23, 2003; revised September 9, 2003. This work was supported by the Engineering and Physical Sciences Research Council under Grant GR/R07844/01.

R. R. A. Syms, H. Zou, and J. Stagg are with the Optical and Semiconductor Devices Group, Electrical and Electronic Engineering Department., Imperial College London, London SW7 2BT, U.K. (e-mail: r.syms@ic.ac.uk).

D. F. Moore is with the Cambridge University Engineering Department, Cambridge CB2 1PZ, U.K.

Digital Object Identifier 10.1109/LPT.2003.820476

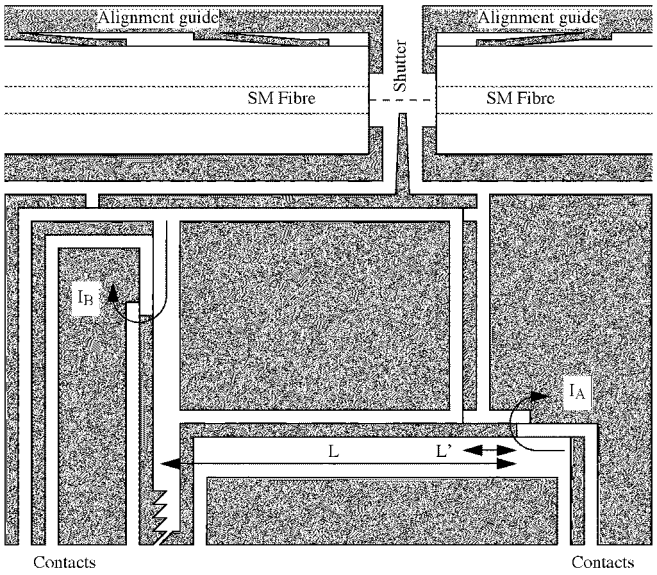

Fig. 2. Layout of a MEMS latching shutter-insertion variable optical attenuator (not to scale).

The shutter and latch levers are ≈7.5 and 2 mm in length, respectively, and 40 μm in width. The actuators have hot and cold arm lengths of 800 μm and 50 μm, respectively, and 5 μm width. The depth and spacing Δ of the rack teeth are both 10 μm, and $L/L' = 10$. The rack is designed to overlap the lever tooth by 10 μm, to provide a clamping force when the latch is closed. A deflection of 20 μm is therefore required to open the latch. Prototypes have been fabricated in BSOI with an 85 μm thick bonded Si layer by DRIE, HF undercut, freeze-drying and sputter-coating with Cr (100 nm) and Au (300 nm) metal. Fig. 3(a), (b), and (c) shows scanning electron microscope views of the shutter, the shutter drive and the latch, respectively. The overall die size is 13.3 mm × 4 mm.

The electromechanical performance of completed devices was first characterized at low frequency by separately applying the currents I_A and I_B. The electrical resistance of the actuators was ≈ 30 Ω. Fig. 4 shows the variation of tip displacement with power for the latch and shutter levers. The variations are quasilinear, and large deflections are obtained at low powers. A 200-μm deflection of the shutter lever was obtained at a drive power of ≈170 mW. This deflection corresponds to ≈ 20-μm motion of the shutter itself, sufficient to cover the attenuation range. Similarly, a 20-μm deflection of the latch lever was obtained at ≈100 mW; this deflection is just sufficient to open the latch. Thermal damage to both actuators occurred at higher powers, typically in excess of 200 mW.

The high-frequency performance was then assessed, by driving the shutter actuator from a sinusoidal source. Fig. 5 shows the variation of peak-to-peak displacement with drive frequency. Because the actuator is power-operated, the mechanical response is at twice the frequency shown. The displacement is approximately constant at low frequencies, but starts to fall as the frequency rises. This feature is characteristic of electrothermal actuators, which are first-order dynamical systems. The 3-dB point is at ≈100 Hz. Two large peaks in deflection may be seen at slightly higher frequencies; these correspond

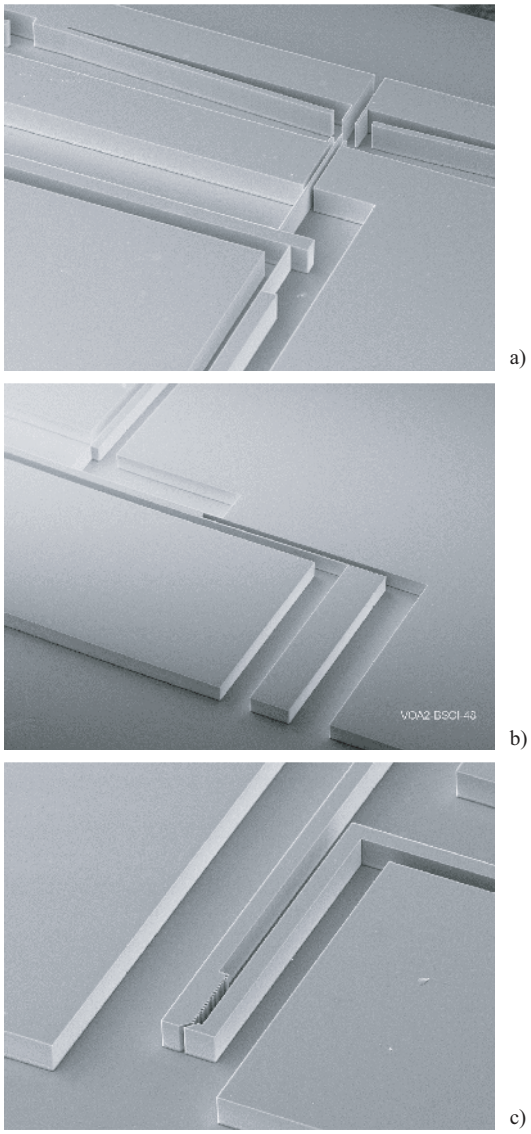

Fig. 3. SEM photographs of (a) the shutter blade and fiber location features, (b) the shutter actuator, and (c) the latch, in a device formed by DRIE of BSOI.

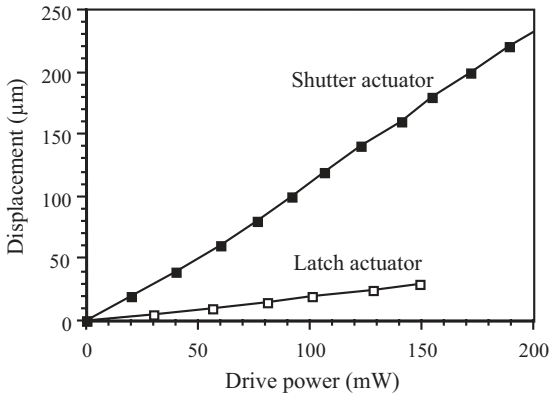

Fig. 4. Variation of deflection with drive power for the shutter and latch levers.

to bending mode resonances of the shutter support beams. The lowest occurs at ≈150 Hz, or a mechanical resonance of $f_n = 300$ Hz. The quality factor (Q-factor) of this resonance is ≈12.3, so that the damping factor is $\zeta = 1/2Q \approx 0.0405$. The

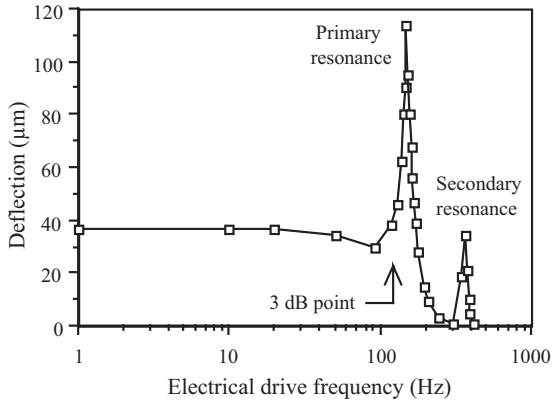

Fig. 5. Variation of deflection with drive frequency, for the shutter lever.

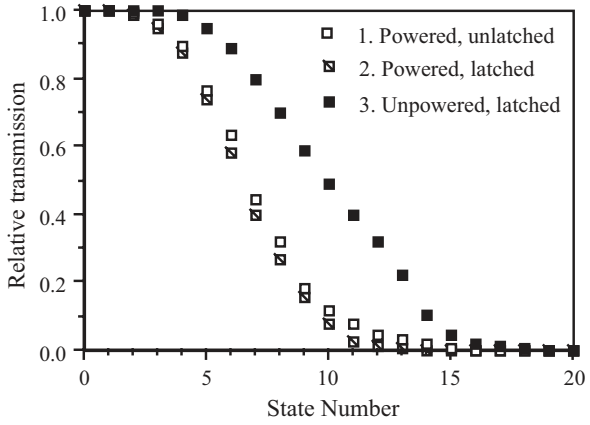

Fig. 6. Measured attenuation achieved when the shutter is 1) powered, but not latched, 2) powered and mechanically latched, and 3) latched, but all drive power is removed.

settling time following a step excitation may then be estimated as $\mathrm{t} = 1/2\pi f_n \zeta = 0.013$ s, or 13 ms.

Cleaved lengths of 8/125 μm single-mode fiber were then inserted into the alignment features, and optical performance was measured using broad band, unpolarized light. The input was connected to an Agilent 83 438A erbium ASE source, operating near 1.55-μm wavelength. The output was detected using a Ge photodiode connected to a transimpedance amplifier. No antireflection coatings or index-matching liquid was used to reduce the fixed insertion loss, which was measured as 1.0–1.5 dB in repeated assembly operations.

The attenuation in the different VOA states was measured under three separate conditions. 1) The latch was opened by applying I_B, and the shutter electrically driven to each possible state by applying various I_A. 2) The shutter was driven as before, but the latch was closed by removing I_B to apply a clamping force to the shutter lever. 3) Power was removed from the shutter actuator, so that it remained latched. Fig. 6 shows the transmission as a function of the state number in each condition, ignoring the fixed insertion loss.

In Condition 1, the transmission decreases monotonically to a low level as the state number rises, and a relative attenuation of (for example) ≈30 dB is achieved at State #17. In Condition 2, the variation is similar, but slightly higher attenuation is obtained, suggesting that the force applied by the clamp moves the shutter further across the optical beam. In Condition 3, the attenuation is considerably lower, implying that elastic relaxation occurs when power is removed from the shutter actuator, which withdraws the shutter slightly from the optical beam. Distinct and repeatable latched states can be set, and an attenuation of ≈30 dB is achieved in State #20. The difference in attenuation between adjacent states varies, increasing from ≈0.2 dB at 1 dB of attenuation to ≈5 dB at 30 dB. There is scope to improve the resolution by a factor of ≈2, since the tooth size (10 μm) is conservative.

The return loss varies across the range, increasing by 9 dB above the value of obtained from the uncoated fiber end as the attenuation rises to 30 dB. This figure could be reduced, by increasing the shutter blade angle and using a cladding mode stripper. The wavelength dependence of the loss (WDL) also increases, from 1.0 dB at 3 dB of attenuation to 6 dB at 30 dB. These values are typical of shutter-insertion VOAs, and could be improved by using the alternative principle of image translation by a moving mirror [9].

Finally, the dynamic response was measured by opening the latch and driving the shutter actuator with a unipolar square wave. Decaying oscillations at the mechanical resonant frequency were superimposed on the expected periodic attenuation variation. From the decay of these oscillations to 1/e of their initial amplitude, the settling time was estimated as 18 msec, in reasonable agreement with the earlier theoretical estimate.

In conclusion, we have demonstrated a multi-state latching MEMS VOA using DRIE and undercut of BSOI. The device can be continuously adjusted or latched into a discrete set of attenuation states using a rack-and-tooth mechanism driven by electrothermal actuators. Initial characterization has shown that performance typical of an analogue moving-shutter VOA may be combined with a latching functionality in a simple geometry.

REFERENCES

[1] C. Marxer, P. Griss, and N. F. de Rooij, "A variable optical attenuator based on silicon micromechanics," *IEEE Photon. Technol. Lett.*, vol. 11, pp. 233–235, Feb. 1999.

[2] C.-H. Ji, Y. Yee, J. Choi, and J.-U. Bu, "Electromagnetic variable attenuator," in *IEEE/LEOS Int. Conf. Optical MEMS*, Lugano, Switzerland, Aug. 20–23, 2002, pp. 49–50.

[3] R. Wood, V. R. Dhuler, and E. A. Hill, "A MEMS variable attenuator," in *IEEE/LEOS Int.Conf. Optical MEMS*, Kauai, HI, Aug. 21–24, 2000, pp. 121–122.

[4] V. R. Dhuler and E. A. Hill, "Microelectromechanical devices having brake assemblies therein to control movement of optical shutters and other movable elements," European Patent EP1 139 141, Oct. 4, 2001.

[5] J. Park, L. L. Chu, A. D. Oliver, and Y. B. Gianchandani, "Bent-beam electrothermal actuators—Part II: linear and rotary microengines," *J. Microelectromech. Syst.*, vol. 10, pp. 247–254, June 2001.

[6] H. Guckel, J. Klein, T. Christenson, K. Skrobis, M. Laudon, and E. G. Lovell, "Thermo-magnetic metal flexure actuators," in *Proc. IEEE Solid-State Sensor and Actuator Workshop*, Hilton Head, SC, June 22–25, 1992, pp. 73–75.

[7] P. Lerch, C. K. Slimane, B. Romanowicz, and P. Renaus, "Modelization and characterization of asymmetrical thermal micro-actuators," *J. Micromech. Microeng.*, vol. 6, pp. 134–137, 1996.

[8] C. S. Pan and W. Hsu, "An electro-thermally and laterally driven polysilicon microactuator," *J. Micromech. Microeng.*, vol. 7, pp. 7–13, 1997.

[9] C. Marxer, B. de Jong, and R. de Rooij, "Comparison of MEMS variable optical attenuator designs," in *IEEE/LEOS Int. Conf. Optical MEMS*, Lugano, Switzerland, Aug. 20–23, 2002, pp. 189–190.